



Importance of dynamics in the finite element prediction of plastic damage of polyethylene acetabular liners under edge loading conditions

Faezeh Jahani^a, Lee W. Etchels^a, Lin Wang^{a,b}, Jonathan Thompson^{a,b}, David Barton^a, Ruth K. Wilcox^a, John Fisher^a, Alison C. Jones^{a,*}

^a Institute of Medical and Biological Engineering, School of Mechanical Engineering, University of Leeds, Leeds, United Kingdom

^b DePuy Synthes Joint Reconstruction, Leeds, United Kingdom

ARTICLE INFO

Keywords:

Hip replacement
Ultra-high molecular weight polyethylene
Finite element
Edge loading
ISO testing

ABSTRACT

After hip replacement, in cases where there is instability at the joint, contact between the femoral head and the acetabular liner can move from the bearing surface to the liner rim, generating edge loading conditions. This has been linked to polyethylene liner fracture and led to the development of a regulatory testing standard (ISO 14242:4) to replicate these conditions. Performing computational modelling alongside simulator testing can provide insight into the complex damage mechanisms present in hard-on-soft bearings under edge loading. The aim of this work was to evaluate the need for inertia and elastoplastic material properties to predict kinematics (likelihood of edge loading) and plastic strain accumulation (as a damage indicator).

While a static, rigid model was sufficient to predict kinematics for experimental test planning, the inclusion of inertia, alongside elastoplastic material, was required for prediction of plastic strain behaviour. The delay in device realignment during heel strike, caused by inertia, substantially increased the force experienced during rim loading (e.g. 600 N static rigid, ~1800 N dynamic elastoplastic, in one case). The accumulation of plastic strain is influenced by factors including cup orientation, swing phase force balance, the moving mass, and the design of the device itself. Evaluation of future liner designs could employ dynamic elastoplastic models to investigate the effect of design feature changes on bearing resilience under edge loading.

1. Introduction

Edge loading conditions can occur in total hip replacements (THR). This is where the contact between the femoral head and the acetabular liner moves from the medial bearing surface to the liner rim and is thought to be due to small levels of instability at the hip joint. Edge loading has been linked to adverse tissue reactions from metal-on-metal wear [1,2], squeaking [3] and fracture [4] of ceramic-on-ceramic devices. The physiological causes for joint instability will vary from patient to patient and event to event. They may be driven by the direction of the resultant hip contact force relative to the liner, by lever-out due to impingement, or by other mechanisms. Gait studies under imaging have shown that separation of the device head and cup (leading to edge loading) can be measured *in vivo* [5], and is prominent for standard, unconstrained metal-on-polyethylene devices [6]. Evidence of edge loading has been seen in clinical device retrievals, including the fracture

of some polyethylene acetabular liners [7].

The need to evaluate potential new devices under edge loading conditions prior to implantation, has driven the development of a regulatory testing standard (ISO 14242:4) [8] to generate edge loading conditions in all but the most constraining hip replacement designs. In these tests, idealised simulation of hip joint gait is modified to include a driver for separation of the acetabular cup and femoral head during the swing phase. An additional spring is attached along the mediolateral (ML) axis, with a pre-set compression (also referred to as the mismatch), which generates a force causing the contact location to move laterally towards the liner rim. During the stance phase the axially applied joint contact force is sufficiently high that the contact location remains within the main bearing surface, but the lower axial load during swing phase allows the mediolateral spring force to translate the contact location towards, and sometimes onto, the liner rim.

Standardised testing has produced evidence of the effects of edge

Abbreviations: THR, total hip replacement; UHMWPE, ultra-high molecular weight polyethylene; FE, finite element; MoP, metal-on-polyethylene; Code PyEL, python edge loading; SwPL, swing phase load; ML, mediolateral.

* Corresponding author.

E-mail address: a.c.jones@leeds.ac.uk (A.C. Jones).

<https://doi.org/10.1016/j.medengphy.2021.07.010>

Received 11 March 2021; Received in revised form 25 June 2021; Accepted 27 July 2021

Available online 12 August 2021

1350-4533/© 2021 The Authors. Published by Elsevier Ltd on behalf of IPREM. This is an open access article under the CC BY license

(<http://creativecommons.org/licenses/by/4.0/>).

loading under controlled conditions [9,10] and shown that these effects are complex for the hard-on-soft bearing combination [11], where the most common acetabular liner material is Ultra High Molecular Weight Polyethylene (UHMWPE). While edge loading conditions have been seen to reduce liner volume change for hard-on-soft bearings in comparison to standard conditions [12], possibly due to differences in both contact area and lubrication conditions, they have also been linked to rim damage and device fracture [11].

Performing computational modelling alongside controlled simulator testing can provide insight into the mechanisms by which damage happens, and aid in designing devices which are better able to withstand edge loading conditions. Static modelling studies have considered deformation and damage and have shown that edge loading led to increased plastic strain [13–15], increased contact pressures [13–17], and increased liner peak von Mises stress [15]. It is also possible that edge loading contributes to disassociation of the acetabular cup from its fixation, with modelling showing the highest torque on the shell occurring at the highest separation [18].

There is a need to develop an improved understanding of the mechanisms underlying edge loading damage, to inform future device design and testing. Dynamic rigid modelling studies have shown that the inclusion of damping effects, such as inertia or friction, increases the peak force transferred through the edge of the cup during heel-strike [19–21]. This additional force is not captured in the studies using static modelling to analyse edge loading effects. Therefore, to fully capture the loads experienced during an edge loading cycle and make predictions about liner stress, contact area, or damage indicators, it seems necessary to combine inertial effects with elastoplastic material properties. To the authors' knowledge no published research paper has combined these effects to investigate the effect of dynamic edge loading kinematics and the additional complexity naturally adds to the computational cost of the enterprise. The aim of this work was to evaluate the need for various levels of complexity in a finite element (FE) model predicting the likelihood and consequences of edge loading conditions in a THR with an UHMWPE liner. The need for a complex model, incorporating both inertia and elastoplastic material properties, was assessed in terms of kinematics and in terms of plastic strain accumulation.

2. Methods

The objectives of this work were: to evaluate the effects of a combination of inertia and material deformation on head-cup separation behaviour, and determine whether this additional complexity is required for accurate prediction of experimental separation behaviour (studies 1 and 2); and to investigate the factors contributing to increases in damage indicators within a dynamic, elastoplastic model, such as kinematics, instantaneous forces and contact location (study 3).

Study 1. A dynamic deformable FE model was compared against both ISO 14242:4 experimental data [22] and a much simpler, static rigid model prediction (Python Edge Loading, PyEL [19]). This served to validate the overall behaviour of the FE model and to establish whether the addition of both inertia and material deformation had any substantial effects on the separation of the head and the cup during swing phase. A set of 32 parametric scenarios were tested, representing a full factorial combination of swing phase load, mediolateral mismatch and inclination angle values. The values tested for each parameter are listed in Table 1.

Study 2. The second study investigated how inertia and deformation could affect the kinematics during portions of the load cycle where they are more difficult to measure and evaluate experimentally (such as heel-strike and toe-off), but where they may have a significant contribution to the accumulated liner damage and wear seen post-test. The kinematics were compared between the full dynamic deformable FE model and the simpler static rigid prediction. This analysis was undertaken for selected cases, with a fixed cup inclination angle of 45° and mismatch (pre-set

Table 1

Details of parametric settings for all cases performed for each different edge loading model. All THR devices had 36 mm metal femoral heads articulating against polyethylene acetabular cups.

	Experiment	PyEL	Dynamic Deformable FE
Mismatch	1–4 mm	1–4 mm	1–4 mm
Swing Phase Load (SwPL)	70, 100, 200, 300 N	70, 100, 200, 300 N	70, 100, 200, 300 N
Inclination	45, 65°	45, 65°	45, 65°
Run Time (per case)		~1 minute	~24 hours

spring compression) level of 4 mm (Table 1) and swing phase loads of 70N and 200N. These cases were selected for detailed analysis due to a relatively large difference in the 200N case between the maximum separations from the two models during study 1.

Study 3. The final study investigated whether the propensity for liner damage could be predicted through correlations to the kinematics alone, or whether explicitly calculating the deformation and damage is required. The relationships between the force scenario, the separation behaviour, the contact mechanics, and the plastic strain were analysed in the dynamic, deformable FE model. Contact pressures and areas were analysed to show the effect of loading on the device rim, peak plastic strain was recorded as a measure of localised damage and geometry change, and the total plastic dissipated strain energy was used as a measure of total damage and geometry change.

All cases used the geometry of a 36mm metal-on-polyethylene (MoP) THR bearing (PINNACLE® MARATHON®, DePuy Synthes, UK), with a neutral liner and a radial clearance of 0.5 mm.

The PyEL model [19], is a static, frictionless, rigid model which calculates the axial forces required to generate 3000 separation positions and reconstructs the load cycle behaviour. The liner geometry was represented by a point cloud generated from a 0.05 mm triangular element surface mesh and the head was modelled as an analytical sphere.

In the dynamic deformable FE model (Fig. 1a), the head was modelled as a rigid body meshed with 1.5 mm linear hexahedral elements ($\rho = 4.37 \times 10^3 \text{ kg/m}^3$). The liner was a deformable body meshed with 1.5mm linear C3D8R hexahedral elements and was given elastoplastic material properties of MARATHON® Cross-linked UHMWPE (linear elastic modulus 677 MPa, yield stress 8.4 MPa). The acetabular shell was meshed with 2mm hexahedral elements, given linear elastic material properties representing titanium alloy ($E = 114.5 \text{ GPa}$, $\nu = 0.34$, $\rho = 4.43 \times 10^3 \text{ kg/m}^3$). The shell was tied into a rigid body cup holder representing the experimental test fixture, with an assigned inertial mass of 2.5kg. Frictionless contact conditions were assumed at the bearing surfaces and a perfectly bonded condition was assumed between the acetabular shell and the liner. The dynamic time increment was

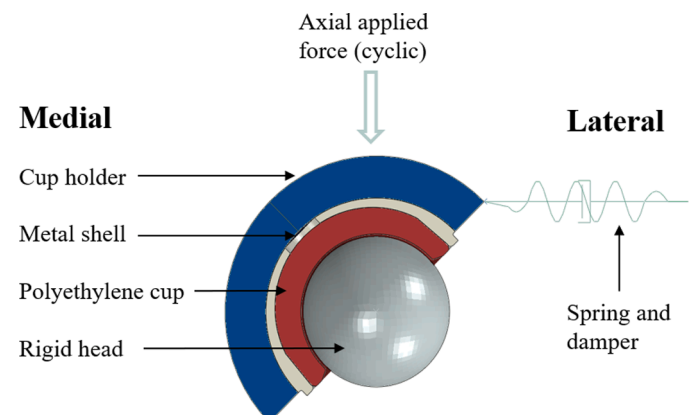


Fig. 1. Schematic of the dynamic deformable finite element model.

globally estimated by the explicit solver (Abaqus v6.14, Dassault Systèmes, France) based on the size and wave speeds of the elements in the model. Mesh sensitivity was performed to produce converged contact areas under direct bearing surface contact [23]. The overall element quality with the polyethylene liner was good (face angles in degrees: average minimum 75, average maximum 105, ideal 90; aspect ratio: average 2.3, ideal 1) and any elements of lower quality were away from the rim area. Further refinement was limited by run time (Table 1). Following the convention in experimental literature [24], cup inclination angles will be given in this paper as the clinical inclination (e.g. a clinical inclination of 45° is implemented in experimental simulation at 35°).

For each combination of input settings, a pre-analysis run was performed where the spring was compressed with the cup constrained in place, and then the cup was released. The damping coefficient was varied until a value representing critical damping was found (quickest return to stable without any oscillation). The test-specific critical damping coefficient was then used for each FE case to maximise solution stability. All cases used a spring stiffness of 100 N/mm.

The main analysis was performed in three steps. Contact within the main bearing surface was established by constraining all ML translation of the cup and applying the swing phase load in the axial direction. The ML constraints were then released, allowing the cup to translate to a separated position. A loading profile representing one cycle used in the experimental testing (at 1 Hz) was then applied.

The experimental data, showing maximum separation of the head and the cup, was taken from a previous study [22]. A hip joint simulator (ProSim EM13, Simulation Solutions, UK) was used along with the protocol from ISO 14242:4 [8]. The hip replacement device and the set of 32 scenarios matched those described above.

3. Results and discussion

The data associated with this paper are openly available from the University of Leeds Data Repository [25].

Study 1: Verification and validation of the dynamic deformable FE separation behaviour

Experimental results suitable for direct comparison were only available for a subset of the cases, as machine and measurement limits precluded accurate separation measurements below a certain threshold, which was variable based on the mismatch [19]. Where comparisons could be made the models replicated the experimental trends. The FE model consistently overestimated the experimental maximum separation (with a mean overestimation of 0.3 mm, Fig. 2). As identified and described in Etchels et al. [19], small amounts of bending and deformation of the simulator fixtures results in a reduction in the effective spring stiffness and the additional compliance reduces the spring compression required to allow for a given separation. Experimentally, the equivalent spring stiffness will therefore be lower than that used in the models and this will be responsible for some of the 0.3 mm

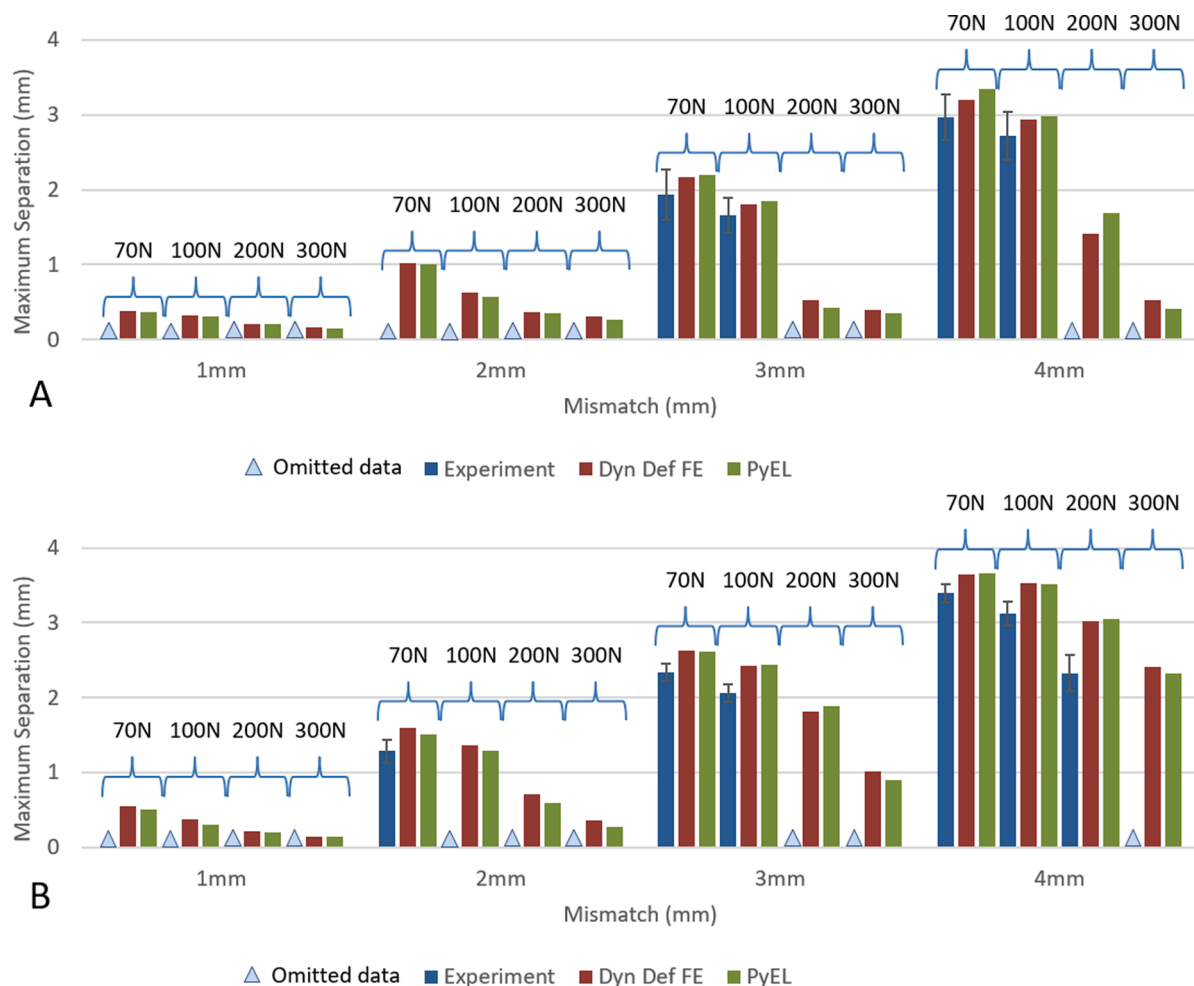


Fig. 2. Comparison of the experimental, dynamic deformable FE, and static rigid PyEL maximum separations at a 45° (A) and 65° (B) clinical inclination angle. Experimental cases where the result was below the measurement sensitivity threshold for each mismatch (0.7, 1.1, 1.6, and 2.1mm for 1, 2, 3, and 4mm mismatches) have been omitted. Experimental values are the mean from three stations. Experimental error bars represent ± 1 SD across those three stations. The numbers above the bar groups indicate the swing phase load applied.

overestimation. Bearing friction in the experimental results would also likely reduce the maximum separation compared to the computational models.

There was good agreement between the dynamic deformable FE model and the static rigid PyEL model, for the measure of maximum separation. Differences between the FE and PyEL models were relatively small compared to the mesh resolution of the FE liner (1.5mm). The lack of a clear trend for the difference between the models may be due to specific rim features, to which the rigid point contact PyEL model is more sensitive.

Study 2: The effect of inertia on through-cycle separation behaviour

The through-cycle separation behaviour from the dynamic deformable and static rigid (PyEL) models were compared to evaluate the combined effects of inertia and deformation (Fig. 3). Where the swing phase load was lower and the resulting separation was higher (Fig. 3A), the effect of inertia, and material and spring damping could be seen in a slower change in separation during heel-strike and toe-off. There were clear differences in terms of the peak load under edge loading conditions at heel-strike. For this device design and inclination angle the contact position was found to move to the edge of the bearing surface at a separation of approximately 0.8 mm. For the static rigid model this occurred at an axial load of approximately 600N, whereas the same separation occurred at an axial load of ~1800N in the dynamic deformable case.

The PyEL model predicted some sharp changes in separation due to movement of the contact location across specific rim features and boundaries of the liner, whereas the inclusion of deformation resulted in smoother transitions. In the deformable model maximum separation values result from a combination of material deformation and sliding

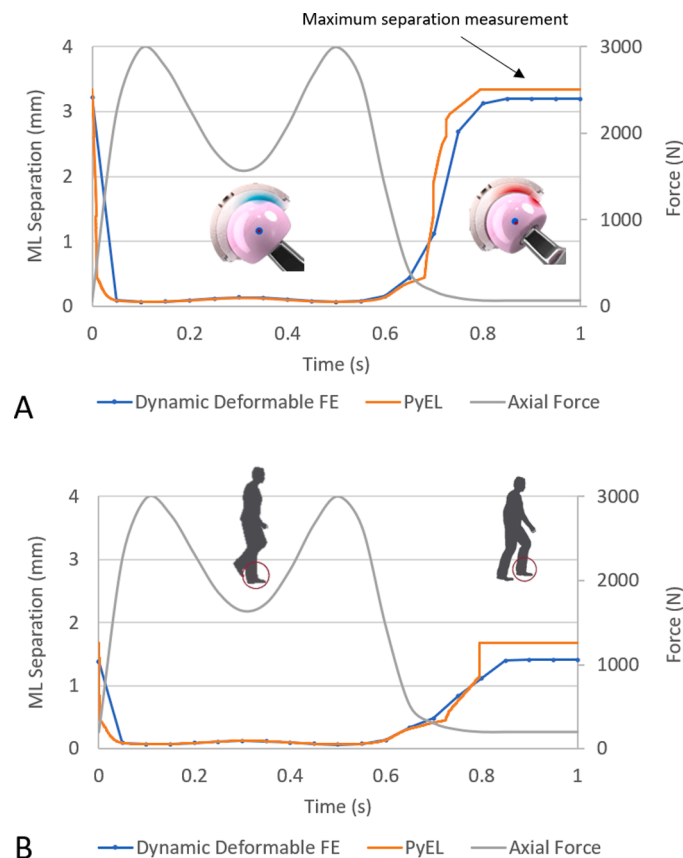


Fig. 3. Comparison of the mediolateral (ML) separation through the gait cycle as predicted by the dynamic deformable finite element model and a static rigid prediction (PyEL). Results given for cases with (A) a 45° clinical inclination, 4mm mismatch, and 70 N swing phase load, and (B) a 45° clinical inclination, 4 mm mismatch, and 200 N swing phase load.

across the rim, with the balance between the two being device and orientation specific. This goes some way to explaining the small differences in maximum separation between the two model types.

Study 3: Prediction of plastic strain in hip device separation testing

Cases where separation was less than ~1 mm maintained a large contact area and avoided plastic strain accumulation (Fig. 4) even under relatively high forces. In cases where the level of separation was sufficient to move the contact towards the cup rim (>1mm) and reduce the contact area, plastic strain accumulation was seen. For convenience these cases will be referred to as having “rim contact”. However, the relationship between maximum separation and plastic strain accumulation was not straight forward and is confounded by several factors.

In cases with rim contact, there were two drivers for additional plastic strain accumulation, namely additional force and additional sliding across the rim. These two mechanisms are illustrated in Fig. 5 where higher contact forces caused the increase in plastic strain accumulation, and in Fig. 6 where additional head-cup separation resulted in the centre of pressure translating further across the rim and causing damage at more locations.

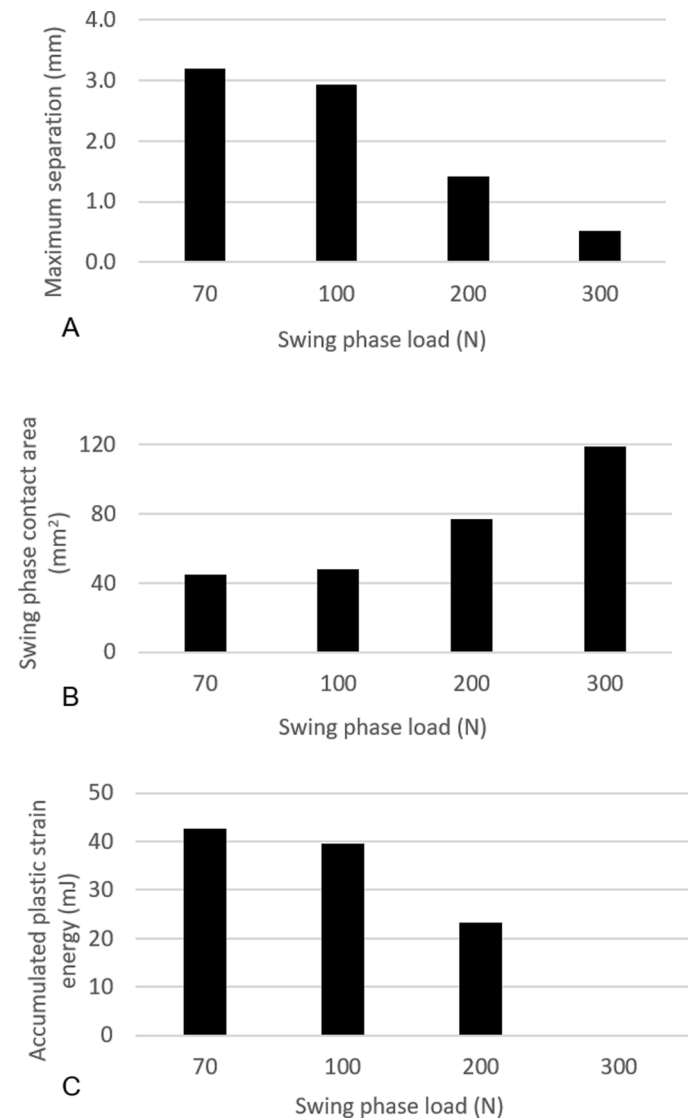


Fig. 4. Maximum separation (A), swing phase contact area (B), and total accumulated plastic strain (C) (represented by the total strain energy dissipated through plasticity) for all swing phase load cases at the 45° clinical inclination angle with a 4 mm mismatch, from the dynamic deformable FE model. (No plastic strain was seen under the highest swing phase load.)

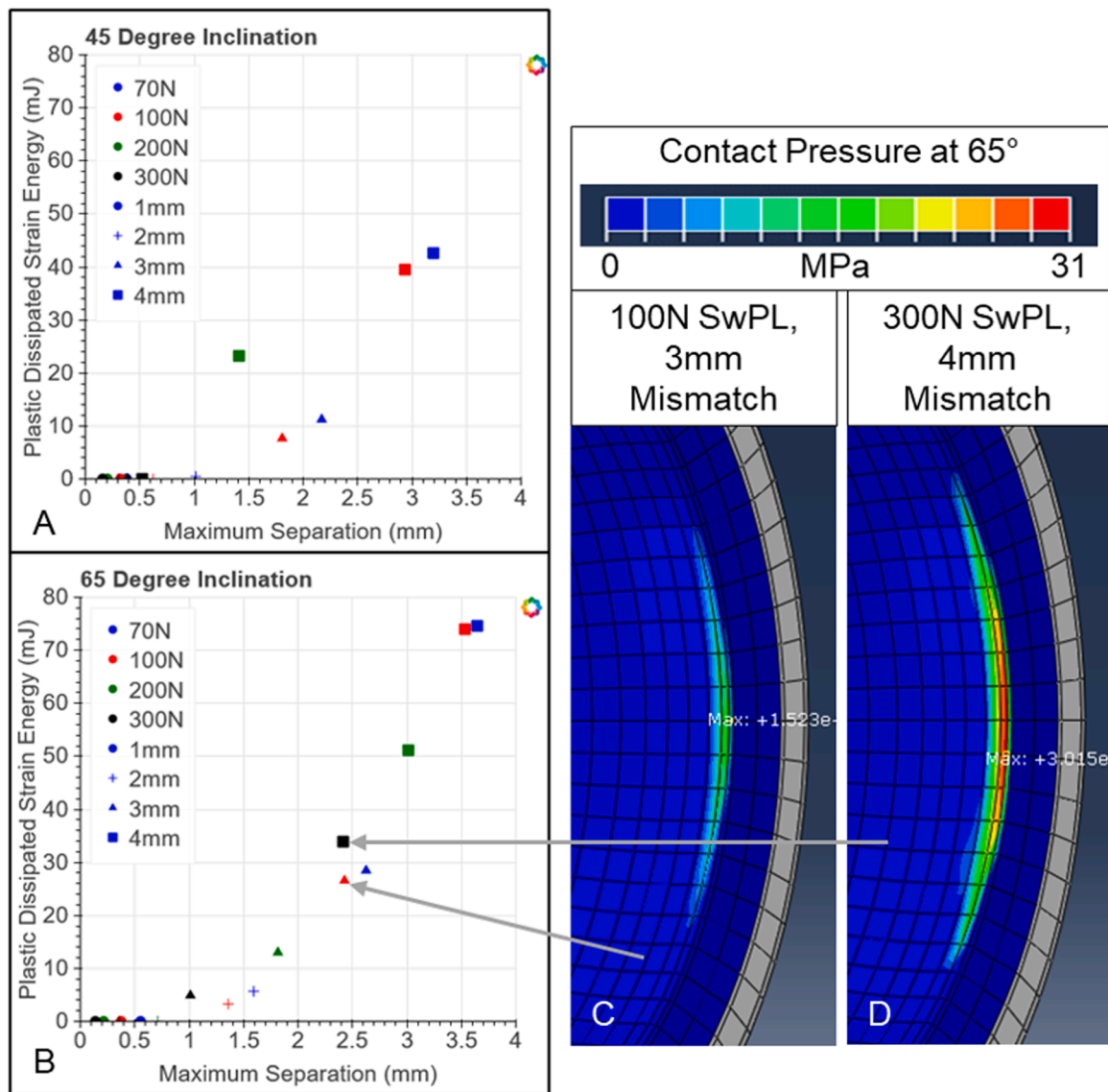


Fig. 5. Left-Relationship between total accumulated plastic strain and maximum separation for all cases, separated by inclination angle, (A) 45°, (B) 65°. Marker colour represents swing phase load (SwPL) and marker shape represents mismatch, as described in legend. Right-FE contact pressure maps at swing phase for two cases with similar maximum separations but dissimilar load environments. (C) 65° inclination, 100 N swing phase load, 3 mm mismatch. (D) 65° inclination, 300 N swing phase load, 4 mm mismatch.

In cases where the (axial) swing phase load was high and the (ML) spring ‘mismatch’ was also high, the head-cup separation may be relatively low, but the resulting high contact force generated additional plastic strain energy (Fig. 5D compared to Fig. 5C). It is therefore possible to generate the same head-cup separation, yet different levels of plastic strain (increase shown in Fig. 5B), due to the contact forces created by the specific combination of swing phase load and mismatch.

The inclination of the cup relative to the axes of the applied loads provided another confounding factor, through two mechanisms. Firstly, a change in cup orientation caused a change in rim position and therefore affected the separation threshold at which rim loading is reached. Secondly, the orientation of the geometry affected the balance of tangential and normal contact forces, and therefore the sliding behaviour on the rim. These effects can be seen in the change of trends between Fig. 5A and 5B.

A reduction in swing phase load was found to generate a wider range of contact locations on the rim, increasing the total accumulated plastic strain in the liner without necessarily increasing the peak plastic strain values. In Fig. 6A, the 300 N swing phase load prevented movement of

the contact to the rim, spreading the contact over a larger area and protecting the liner from yielding. A reduction of the swing phase load to 200 N (Fig. 6B) moved the contact to the rim and initiated plastic damage. Reducing the swing phase load further, to 70 N (Fig. 6C), resulted in further sliding and additional yielding of the newly contacted UHMWPE with little effect on the previously damaged regions.

Due to analysis time constraints, and a runtime of ~24 hours per case, the dynamic deformable models presented in this study were restricted in mesh resolution. For detailed liner stress and strain information suitable for direct comparison to failure criteria, beyond the analysis of trends and mechanisms, further optimisation and development of the model will be needed to balance precision with computational cost.

4. Conclusion

The dynamic deformable FE model of edge loading developed in this work was verified through comparison to a simple static rigid model and validated by comparison to experimental test data. The trends in

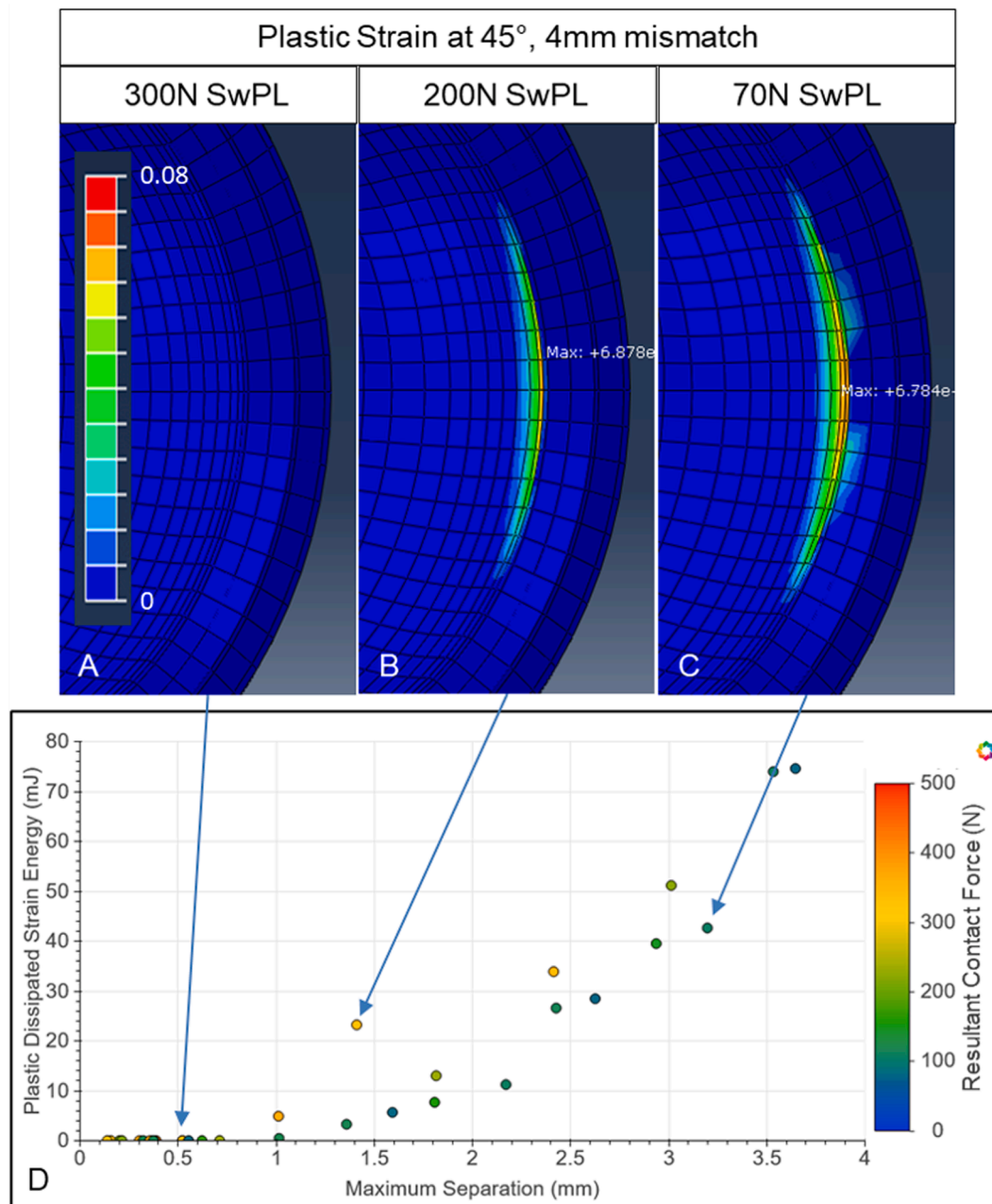


Fig. 6. Top-FE plastic strain maps at end of test for three different swing phase load (SwPL) cases that created three different maximum separations. (A) 300 N, (B) 200 N, (C) 70 N. All cases used 45° inclination and 4mm mismatch. Bottom-All cases, from both inclination angles, by maximum separation, total accumulated plastic strain, and resultant contact force at swing phase (by colour). Specific cases shown in A, B, and C indicated by arrows onto D.

maximum bearing separation with different input case parameters (force environments and orientations) could be well replicated by both the dynamic deformable FE model and the simple static rigid model. Given an aim of predicting separation behaviour for experimental test planning, there are some disadvantages to a static rigid modelling approach for hard-on-soft bearings, as it can overestimate the importance of specific rim geometry features and edges, which in a deformable model will be smoothed out within the contact area. However, dynamic deformable FE models of edge loading have limited advantage and a significant increase in analysis time for experimental pre-test planning focused on estimations of the maximum separation alone, and static rigid models are sufficient for that task.

In order to analyse the potential for acetabular liner damage under edge loading it is necessary to include an elastoplastic material model. When that material model is integrated into a dynamic model the

computational cost and complexity increases substantially, making it important to demonstrate the necessity of the dynamic aspect. The inclusion of inertia was shown to modify timing of the beginning and end of edge loading, which delayed both separation during toe off and relocation at heel strike. In some cases, the delay at heel strike generated a load on the rim of three times that of the static case. This increase in the contact force experienced during edge loading could have substantial implications for predictions of liner damage and is therefore important to capture.

Understanding the mechanisms behind the damage to UHMWPE liners, both *in vitro* and *in vivo*, under edge loading conditions can be aided by dynamic, elastoplastic FE models that capture in combination the differences between load cases and liner designs. In this work, plastic strain in the liner was increased either by the generation of higher strains under the contact through increased contact force, or by

sweeping the contact over a larger portion of the rim. These are mechanisms that could also be induced by device design feature changes. Optimisation and evaluation of future liner designs may benefit from the use of dynamic deformable FE models to investigate the effect of design feature changes on bearing resilience under edge loading.

Ethical approval

Not required.

Declaration of Competing Interest

JT and LW are employees of DePuy Synthes Joint Reconstruction, Leeds, United Kingdom. JF has acted as a paid consultant and has provided paid expert testimony for DePuy Synthes.

Funding

FJ was supported by a UKRI EPSRC CASE studentship with DePuy Synthes Joint Reconstruction (Leeds, UK). This work is supported in part by UKRI EPSRC Healthcare Impact Partnership Grant (EP/N02480X/1) and by the National Institute for Health Research (NIHR) Leeds Biomedical Research Centre (BRC). JF was supported by UKRI EPSRC as Director of the Medical Technologies Innovation and Knowledge Centre.

References

- [1] Mellon SJ, Kwon YM, Glyn-Jones S, Murray DW, Gill HS. The effect of motion patterns on edge-loading of metal-on-metal hip resurfacing. *Med Eng Phys* 2011; 33:1212–20. <https://doi.org/10.1016/j.medengphy.2011.05.011>.
- [2] Kovochich M, Fung ES, Donovan E, Unice KM, Paustenbach DJ, Finley BL. Characterization of wear debris from metal-on-metal hip implants during normal wear versus edge-loading conditions. *J Biomed Mater Res B Appl Biomater* 2018; 106:986–96. <https://doi.org/10.1002/jbm.b.33902>.
- [3] Glaser D, Komistek RD, Cates HE, Mahfouz MR. Clicking and squeaking: *in vivo* correlation of sound and separation for different bearing surfaces. *J Bone Jt Surg* 2008;90:112–20. <https://doi.org/10.2106/JBJS.H.00627>. Am.
- [4] Stewart TD, Tipper JL, Inasley G, Streicher RM, Ingham E, Fisher J. Severe wear and fracture of zirconia heads against alumina inserts in hip simulator studies with microseparation. *J Arthroplast* 2003;18:726–34. [https://doi.org/10.1016/s0883-5403\(03\)00204-3](https://doi.org/10.1016/s0883-5403(03)00204-3).
- [5] Dennis DA, Komistek RD, Northcutt EJ, Ochoa JA, Ritchie A. *In vivo* determination of hip joint separation and the forces generated due to impact loading conditions. *J Biomech* 2001;34:623–9.
- [6] Komistek RD, Dennis DA, Ochoa JA, Haas BD, Hammill C. *In vivo* comparison of hip separation after metal-on-metal or metal-on-polyethylene total hip arthroplasty. *J Bone Jt Surg* 2002;84:1836–41. Am-A.
- [7] Furmanski J, Anderson M, Bal S, Greenwald AS, Halley D, Penenberg B, Ries M, Pruitt L. Clinical fracture of cross-linked UHMWPE acetabular liners. *Biomaterials* 2009;30:5572–82.
- [8] International Organisation for Standards, ISO 14242-4:2018 Implants for surgery-wear of total hip-joint prostheses, <https://www.iso.org/standard/63835.html> accessed 12 May 2021.
- [9] O'Dwyer Lancaster-Jones O, Williams S, Jennings LM, Thompson J, Isaac GH, Fisher J, Al-Hajjar M. An *in vitro* simulation model to assess the severity of edge loading and wear, due to variations in component positioning in hip joint replacements. *J Biomed Mater Res Part B Appl Biomater* 2018;106B:1897–906.
- [10] Manaka M, Clarke IC, Yamamoto K, Shishido T, Gustafson A, Imakiire A. Stripe wear rates in alumina THR-comparison of microseparation simulator study with retrieved implants. *J Biomed Mater Res Part B Appl Biomater* 2004;69:149–57. <https://doi.org/10.1002/jbm.b.20033>.
- [11] Partridge S, Tipper JL, Al-Hajjar M, Isaac GH, Fisher J, Williams S. Evaluation of a new methodology to simulate damage and wear of polyethylene hip replacements subjected to edge loading in hip simulator testing. *J Biomed Mater Res B Appl Biomater* 2018;106:1456–62. <https://doi.org/10.1002/jbm.b.33951>.
- [12] Williams S, Butterfield M, Stewart T, Ingham E, Stone M, Fisher J. Wear and deformation of ceramic-on-polyethylene total hip replacements with joint laxity and swing phase microseparation. *Proc Inst Mech Eng H* 2003;217:147–53.
- [13] Donaldson FE, Nyman E, Coburn JC. Prediction of contact mechanics in metal-on-metal total hip replacement for parametrically comprehensive designs and loads. *J Biomech* 2015;48:1828–35. <https://doi.org/10.1016/j.jbiomech.2015.04.037>.
- [14] Liu F, Williams S, Fisher J. Effect of microseparation on contact mechanics in metal-on-metal hip replacements-a finite element analysis. *J Biomed Mater Res B Appl Biomater* 2015;103:1312–9. <https://doi.org/10.1002/jbm.b.33313>.
- [15] Hua X, Li J, Wang L, Jin Z, Wilcox R, Fisher J. Contact mechanics of modular metal-on-polyethylene total hip replacement under adverse edge loading conditions. *J Biomech* 2014;47:3303–9. <https://doi.org/10.1016/j.jbiomech.2014.08.015>.
- [16] Mak MM, Besong AA, Jin ZM, Fisher J. Effect of microseparation on contact mechanics in ceramic-on-ceramic hip joint replacements. *Proc Inst Mech Eng H* 2002;216:403–8.
- [17] Sariali E, Stewart T, Jin Z, Fisher J. Effect of cup abduction angle and head lateral microseparation on contact stresses in ceramic-on-ceramic total hip arthroplasty. *J Biomech* 2012;45:390–3. <https://doi.org/10.1016/j.jbiomech.2011.10.033>.
- [18] Liu F, Williams S, Jin Z, Fisher J. Effect of head contact on the rim of the cup on the offset loading and torque in hip joint replacement. *Proc Inst Mech Eng H* 2013;227:1147–54. <https://doi.org/10.1177/0954411913496016>.
- [19] Etchells L, Wang L, Al-Hajjar M, Williams S, Thompson J, Isaac G, Wilcox R, Jones A. Computationally efficient modelling of hip replacement separation due to small mismatches in component centres of rotation. *J Biomech* 2019;95. <https://doi.org/10.1016/j.jbiomech.2019.07.040>.
- [20] Leng J, Al-Hajjar M, Wilcox R, Jones A, Barton D, Fisher J. Dynamic virtual simulation of the occurrence and severity of edge loading in hip replacements associated with variation in the rotational and translational surgical position. *Proc Inst Mech Eng H* 2017;231:299–306. <https://doi.org/10.1177/0954411917693261>.
- [21] Liu F, Feng L, Wang J. A computational parametric study on edge loading in ceramic-on-ceramic total hip joint replacements. *J Mech Behav Biomed Mater* 2018;83:135–42. <https://doi.org/10.1016/j.jmbmb.2018.04.018>.
- [22] Ali M, Al-Hajjar M, Jennings LM, Fisher J. Wear and deformation of metal-on-polyethylene hip replacements under edge loading conditions due to variations in surgical positioning. *Orthop Proc* 2018;99-B:12.
- [23] Jahani F. Modelling of dynamic edge loading in total hip replacements with ceramic on polyethylene bearings, PhD Thesis, University of Leeds, 2017.
- [24] Leslie IJ, Williams S, Isaac G, Ingham E, Fisher J. High cup angle and microseparation increase the wear of hip surface replacements. *Clin Orthop Relat Res* 2009;467:2259–65. <https://doi.org/10.1007/s11999-009-0830-x>.
- [25] Jahani F, Etchells LW, Wang L, Thompson J, Barton D, Wilcox RK, et al. Dataset supporting the publication "Importance of dynamics in the finite element prediction of plastic damage of polyethylene acetabular liners under edge loading conditions. University of Leeds; 2021. <https://doi.org/10.5518/971>.